URSI AP-RASC, Sydney, Australia, 17 – 22 August 2025

Whistler-Mode Wave Duct Propagation Caused by ULF Wave: Ray-Tracing Simulations and Cluster Observations

Kohki Tachi(1), Yuto.Katoh(1), Ondřej Santolík (2) ,Atsushi.Kumamoto(1), Fuminori.Tsuchiya (1)and Yasumasa Kasaba(1)
(1) Department of Geophysics, Graduate School of Science, Tohoku University, Sendai, Japan
(2) Institute of Atmospheric Physics, Czech Academy of Sciences, Prague, Czech Republic

Abstract

Whistler-mode chorus waves are vital in magnetospheric dynamics, influencing radiation belt electrons. Ducting guides these waves to high latitudes, traditionally attributed to density ducts. This study explores magnetic ducts formed by ULF waves, hypothesizing their role in whistler-mode wave ducting. Ray-tracing simulations using a ULF-based magnetic duct model are validated with Cluster observations. Simulations show ULF wave phase-dependent refractive index variations ducting whistler-mode waves, altering the frequency and wave normal angle characteristics. Cluster data from February 2019 reveal chorus intensity enhancements linked to ULF wave compressional oscillations around the wave phase corresponding to refractive index increases. Observed wave normal angles and ray-tracing results, using observationally constrained ducts, agree with ducting theory. These findings demonstrate ULF wave-driven ducting of chorus waves and reveal a generation process of ducts. This study reveals a key wave propagation mechanism in the magnetosphere and enhances our understanding of wave-particle interactions in the radiation belt dynamics.

1. Introduction

This study investigates whistler-mode wave ducting by ULF waves using ray-tracing simulations, validated with Cluster observations. Whistler-mode chorus waves, common in the magnetosphere (appear in the spectra in the frequency range corresponding to 0.1 - 0.8 Ω_{e0}, where Ω_{e0} represents the electron gyro-frequency of at the magnetic equator) [1], are generated near the magnetic equator through the nonlinear wave-particle interaction [2], [3]. Cyclotron resonance with electrons contributes to wave generation, electron acceleration, and precipitation. With high-latitude propagation, the cyclotron resonance energy reaches relativistic energies [4] and resonates with radiation belt electrons [5-7].

Duct guides chorus waves to high latitudes (Smith et al., 1960) with tube-like refractive index structures. Duct sizes vary, as shown by simulations [8, 9] and observations [11, 12]. While most studies focus on density ducts, magnetic ducts from magnetic field variations have been proposed [13].

We hypothesize that ULF waves form ducts, as their compressional components modulate the background magnetic field, because the whistler-mode refractive index depends on electron density and magnetic field:

$$n_{ref} = \frac{\omega_p^2}{\left(\omega(\Omega_e \cos\theta - \omega)\right)^{1/2}} \tag{1}$$

where ω_p is the plasma frequency, ω is the frequency of whistler-mode wave, Ω_e is the gyro-frequency, and θ is the wave normal angle of whistler-mode wave. Considering Pc4-5 ULF wave periods (45-600 s) [14] and the time scale of chorus propagation in the magnetosphere, ULF ducts are nearly static for chorus waves.

This study uses ray-tracing with a ULF-based magnetic duct model to investigate whistler-mode wave propagation and substantiates by data analysis observed by the Cluster satellite.

2. Ray-tracing simulation

Ray-tracing in the present study uses a modified Kimura (1966) [15] code with a module to represent duct structure in the magnetosphere [16]. The duct structure, defined by L-value width, is generated by ULF wave compressional components. Based on observations [17] and density duct models[8,9], we model the magnetic field including a duct:

$$B_d = B_0\left(1 + \frac{B_\mu}{B_0}\right)^g \tag{2}$$

$$g = \exp\left[-\frac{(L - L_d)^2}{\sigma^2}\right] \tag{3}$$

Here, B_0 is the background field, B_μ is the compressional component, L_d is the duct center L-value, and σ defines the duct width. For the ULF wave model, we use a cold plasma approximation [18, 19] assuming a poloidal wave [20].

Figure 1a shows ULF wave components. The compressional component varies with phase t (T_0: ULF wave period), affecting the refractive index. Figure 1b shows the compressional component ratio (2.5% at the equator). Figure 1c shows the refractive index distribution ($L = 6,\ \sigma = 75/6371.2$).

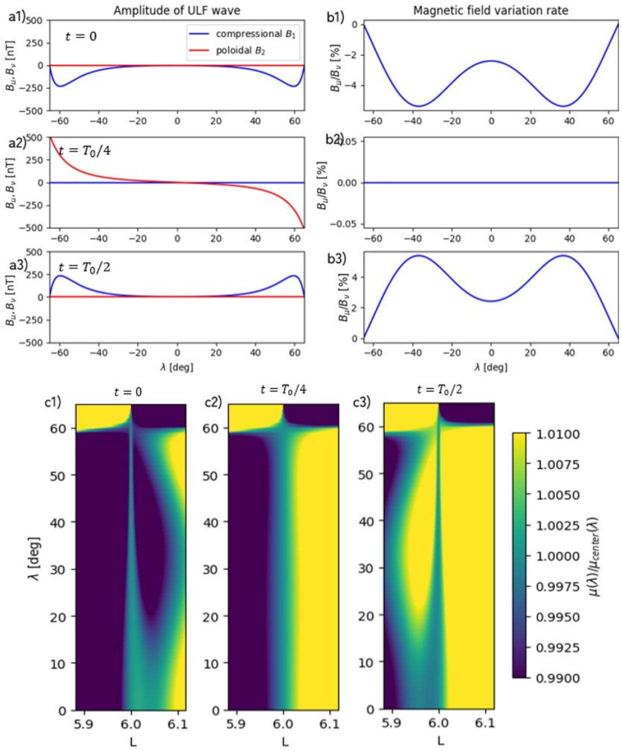

Figure 1. (a) the wave forms of the compressional and poloidal wave. (b) the ration of the compressional component amplitude to the background magnetic field. (c) the refractive index distribution normalized by the refractive index at the duct center.

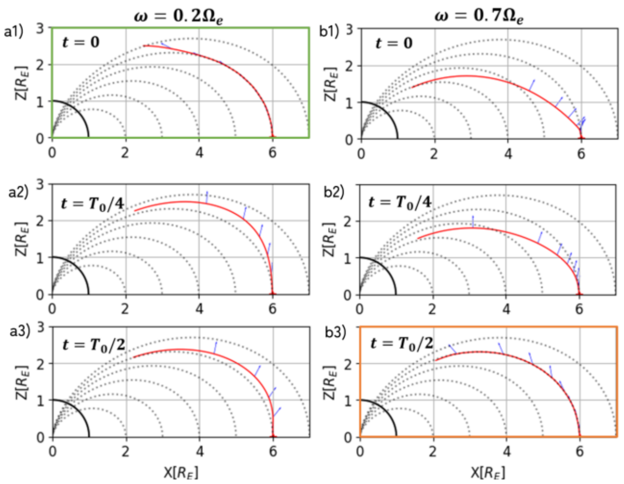

Figure 2. The results of the ray-tracing simulation for (a) 0.2 and (b) 0.7 gyro frequency at the magnetic equator. The red lines show the wave trajectory, and the blue arrows show the wave vectors.

Figure 2 shows ray-tracing results. The red lines are trajectories, and the blue arrows are wave vectors. Calculations were performed for 0.2 and 0.7 Ω_e waves. In Figures 2a1 and 2b3, the whistler-mode waves propagate along the magnetic field lines within the duct structure. In Figure 2a1, the wave vector is oriented along the magnetic field lines, indicating that the whistler-mode wave is propagating quasi-parallel with a small wave normal angle within the duct structure where the refractive index is increased. In contrast, in Figure 2b3, the wave normal angle corresponds to the Gendrin angle [21] and, since the group velocity is directed parallel to the magnetic field lines, the whistler-mode wave is propagating quasi-parallel within the duct structure where the refractive index is decreased. These tendencies are similar to theoretical expectations [22].

We modeled the duct structure caused by ULF waves and performed ray-tracing simulations to demonstrate the possibility of ducting propagation by ULF waves. We also clarified the propagation characteristics of ducted whistler-mode waves depending on the phase of the ULF wave.

3. Event analysis

This event analysis demonstrates ULF wave ducting using Cluster data observed on February 15, 2019 (02:10-02:30 UT) at L=6.5, MLT=3.2, and 20 degrees latitude.

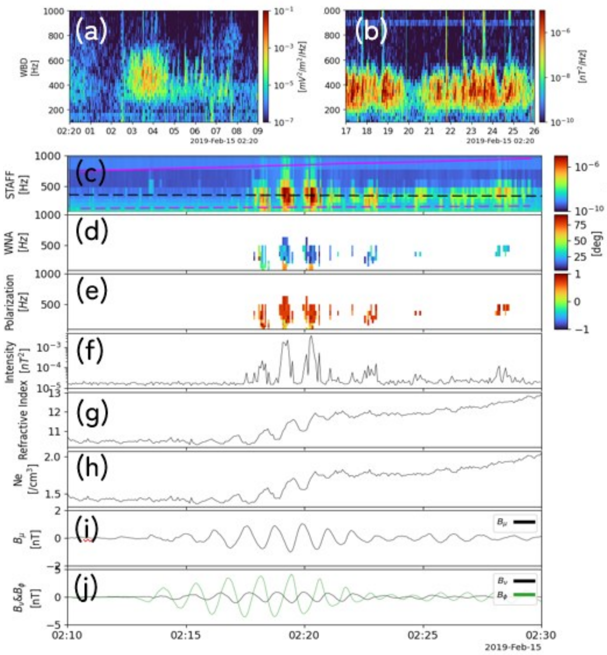

Figure 3. Cluster satellite observation data. (a-b) WBD spectrograms. (c-e) STAFF spectrogram and SVD analysis results. (f) Chorus intensity. (g) Refractive index. (h) Electron density. (i-j) ULF waves.

Figures 3a-b show WBD spectrograms with rising-tone chorus generated near the magnetic equator via nonlinear wave-particle interaction [1, 3, 23]. Figure 3c shows the magnetic field component of the spectra measured by STAFF, including the frequency range corresponding to the lower-band chorus near the equator (the magenta lines indicate 0.1 and 0.5 Ω_{e0}) based on the results of the field line tracing by the Tsyganenko model [24]. Figures 3i-j show ULF wave magnetic field oscillations for each component, B_ϕ is toroidal, B_ν is poloidal, and B_μ is compressional component. Figure 3h shows anti-phase electron density variations to the compressional component of the ULF wave. The refractive index (Figure 3g) and chorus intensity (Figure 3f) correlate well. Figure 3d shows wave normal angles < 40 degrees, and Figure 3e shows right-hand polarization, calculated with the singular value decomposition method [25]. Observed waves (less than half of the local cyclotron frequency) propagate quasi-parallel, consistent with ducting conditions [22].

Ray-tracing used an observation-based duct model (135.88 km width, 15.9% density, -1.5% magnetic field change, L=6.5). The initial wave position was at the equator with 0-degree angle. Figure 4a shows the simulation result of the 0.2 Ω_{e0}. Trajectories (red) and wave vectors (blue) show quasi-parallel propagation along L=6.5. Figure 4b shows the wave normal angles and displacements from the duct center, consistent with the ducting whistler-mode wave [22].

Figure 4c shows maximum wave normal angles for various frequencies. Lower frequency waves are ducted to higher latitudes. Figure 4d compares observed wave normal angles (black dots) with theoretical maximum angles based on the observed refractive index variation (red line) and ray-tracing results demonstrating duct propagation (blue line), they show the consistent result supporting duct propagation caused by ULF wave.

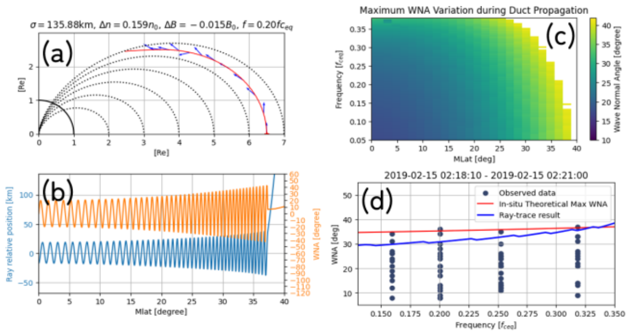

Figure 4. The results of ray-tracing simulation with the observation-based duct model and comparison with the observation. Calculated whistler-mode wave of 0.2 $\Omega_{e,eq}$ (a) trajectory (red line) and wave number vectors direction (blue arrows), and (b) WNA (orange) and displacement (blue) from duct center. (c) Maximum WNA for each frequency and magnetic latitude. (d) Observed WNA (black dots), theoretical maximum WNA based on the observed magnetic field and electron density variation, and maximum WNA based on the ray-tracing simulation.

4. Summary and Discussion

This study demonstrates the possibility of whistler-mode wave ducting by ULF waves using ray-tracing simulations. The ULF wave phase affects refractive index variations, leading to different frequencies and wave normal angles for ducted whistler-mode waves.

Cluster observations show chorus waves propagating from the equator to 20 degrees latitude, with intensity variations linked to the simultaneously observed ULF wave compressional component. Anti-phase density variations were also observed. The observed wave normal angles agree with the estimated maximum wave normal angles based on density and magnetic field changes. Furthermore, the ray-tracing calculations using an observation-based duct model also align with observed and theoretical values.

These findings, combining Cluster data analysis and ray-tracing simulations, provide evidence for ULF wave-driven ducting. ULF wave-modulated precipitation of quasi-relativistic electrons and ionospheric TEC have been reported [5, 26]. These phenomena can be explained by ULF wave-induced duct propagation. The spatial structure of ducts is thought to be related to patchy aurora [27]. Considering ULF wave-induced duct propagation, aurora modulated by ULF wave periods may be observed. This study provides new perspectives on the roles of duct propagation and ULF waves in wave-particle interaction in the radiation belt and magnetosphere-ionosphere coupling.

Acknowledgements

This study is supported by JSPS KAKENHI Grants JP18H03727, JP21H04520, JP23H01229 and JP23H05429. This study uses computational resources of the KDK computer system at the Research Institute for Sustainable Humanosphere, Kyoto University, and the HPCI system provided by the Research Institute for Information Technology, Kyushu University, and the Cyberscience Center, Tohoku University, through the HPCI System Research Project (Project IDs: hp210022, hp220040 and hp230046). This research is also supported by the “Computational Joint Research Program (Collaborative Research Project on Computer Science with High-Performance Computing)” and by the joint research program of the Institute for Space-Earth Environmental Research, Nagoya University. This work is also supported by The International Joint Graduate Program in Earth and Environmental Sciences, Tohoku University (GP-EES). We appreciate the WBD, STAFF, MGF, PEACE, and RAPID teams of the Cluster mission and the OMNI team for making data available. We also acknowledge discussions of ERG science team members.

References

[1] O. Santolík, D. A. Gurnett, J. S. Pickett, M. Parrot, and N. Cornilleau-Wehrlin, “Spatio-temporal structure of storm-time chorus,” *J. Geophys. Res. Space Phys.*, vol. 108, no. A7, 2003, doi: 10.1029/2002JA009791.
[2] Y. Omura, Y. Katoh, and D. Summers, “Theory and simulation of the generation of whistler-mode chorus,” *J. Geophys. Res. Space Phys.*, vol. 113, no. A4, 2008, doi: 10.1029/2007JA012622.
[3] Y. Katoh and Y. Omura, “Computer simulation of chorus wave generation in the Earth’s inner

magnetosphere," *Geophys. Res. Lett.*, vol. 34, no. 3, 2007, doi: 10.1029/2006GL028594.
[4] D. Summers, R. M. Thorne, and F. Xiao, "Relativistic theory of wave-particle resonant diffusion with application to electron acceleration in the magnetosphere," *J. Geophys. Res. Space Phys.*, vol. 103, no. A9, pp. 20487–20500, 1998, doi: 10.1029/98JA01740.
[5] A. V. Artemyev *et al.*, "Role of Ducting in Relativistic Electron Loss by Whistler-Mode Wave Scattering," *J. Geophys. Res. Space Phys.*, vol. 126, no. 11, p. e2021JA029851, 2021, doi: 10.1029/2021JA029851.
[6] L. Chen, A. W. Breneman, Z. Xia, and X. Zhang, "Modeling of Bouncing Electron Microbursts Induced by Ducted Chorus Waves," *Geophys. Res. Lett.*, vol. 47, no. 17, p. e2020GL089400, 2020, doi: 10.1029/2020GL089400.
[7] Y. Miyoshi *et al.*, "Penetration of MeV electrons into the mesosphere accompanying pulsating aurorae," *Sci. Rep.*, vol. 11, no. 1, p. 13724, Jul. 2021, doi: 10.1038/s41598-021-92611-3.
[8] M. Hanzelka and O. Santolík, "Effects of Ducting on Whistler Mode Chorus or Exohiss in the Outer Radiation Belt," *Geophys. Res. Lett.*, vol. 46, no. 11, pp. 5735–5745, 2019, doi: 10.1029/2019GL083115.
[9] Y. Katoh, "A simulation study of the propagation of whistler-mode chorus in the Earth's inner magnetosphere," *Earth Planets Space*, vol. 66, no. 1, p. 6, Apr. 2014, doi: 10.1186/1880-5981-66-6.
[11] J. r. Woodroffe and A. v. Streltsov, "Whistler propagation in the plasmapause," *J. Geophys. Res. Space Phys.*, vol. 118, no. 2, pp. 716–723, 2013, doi: 10.1002/jgra.50135.
[12] R. Chen *et al.*, "In Situ Observations of Whistler-Mode Chorus Waves Guided by Density Ducts," *J. Geophys. Res. Space Phys.*, vol. 126, no. 4, p. e2020JA028814, 2021, doi: 10.1029/2020JA028814.
[13] A. V. Streltsov and S. A. Nejad, "Whistler-Mode Waves in Magnetic Ducts," *J. Geophys. Res. Space Phys.*, vol. 128, no. 8, p. e2023JA031716, 2023, doi: 10.1029/2023JA031716.
[14] J. Jacobs, Y. Kato, S. Matsushita, and V. Troitskaya, "Classification of Geomagnetic Micropulsations," *Geophys. J. R. Astron. Soc.*, vol. 8, pp. 341–342, Apr. 2007, doi: 10.1111/j.1365-246X.1964.tb06301.x.
[15] I. Kimura, "Effects of Ions on Whistler-Mode Ray Tracing," *Radio Sci.*, vol. 1, no. 3, pp. 269–284, 1966, doi: 10.1002/rds196613269.
[16] K. Tachi and Y. Katoh, "Formation of a magnetic duct by the compressional component of ULF oscillation: a ray tracing study of whistler-mode wave propagation," *Earth Planets Space*, vol. 76, no. 1, p. 166, Dec. 2024, doi: 10.1186/s40623-024-02109-1.
[17] S. Schäfer *et al.*, "Spatio-temporal structure of a poloidal Alfvén wave detected by Cluster adjacent to the dayside plasmapause," *Ann. Geophys.*, vol. 26, pp. 1805–1817, Jun. 2008, doi: 10.5194/angeo-26-1805-2008.
[18] A. N. Wright, "Asymptotic and time-dependent solutions of magnetic pulsations in realistic magnetic field geometries," *J. Geophys. Res. Space Phys.*, vol. 97, no. A5, pp. 6439–6450, 1992, doi: 10.1029/91JA02666.
[19] R. Rankin, "Auroral density fluctuations on dispersive field line resonances," *J. Geophys. Res. Space Phys.*, vol. 104, no. A3, pp. 4399–4410, 1999, doi: 10.1029/1998JA900106.
[20] C. Wang *et al.*, "Poloidal Mode Wave-Particle Interactions Inferred From Van Allen Probes and CARISMA Ground-Based Observations," *J. Geophys. Res. Space Phys.*, vol. 123, no. 6, pp. 4652–4667, 2018, doi: 10.1029/2017JA025123.
[21] R. Gendrin, "Le guidage des whistlers par le champ magnetique," *Planet. Space Sci.*, vol. 5, no. 4, pp. 274–282, Aug. 1961, doi: 10.1016/0032-0633(61)90096-4.
[22] R. L. Smith, R. A. Helliwell, and I. W. Yabroff, "A theory of trapping of whistlers in field-aligned columns of enhanced ionization," *J. Geophys. Res. 1896-1977*, vol. 65, no. 3, pp. 815–823, 1960, doi: 10.1029/JZ065i003p00815.
[23] Y. Katoh and Y. Omura, "Electron hybrid code simulation of whistler-mode chorus generation with real parameters in the Earth's inner magnetosphere," *Earth Planets Space*, vol. 68, no. 1, p. 192, Nov. 2016, doi: 10.1186/s40623-016-0568-0.
[24] N. A. Tsyganenko and M. I. Sitnov, "Modeling the dynamics of the inner magnetosphere during strong geomagnetic storms," *J. Geophys. Res. Space Phys.*, vol. 110, no. A3, 2005, doi: 10.1029/2004JA010798.
[25] O. Santolík, M. Parrot, and F. Lefeuvre, "Singular value decomposition methods for wave propagation analysis," *Radio Sci.*, vol. 38, no. 1, 2003, doi: 10.1029/2000RS002523.
[26] Y. Shen *et al.*, "Magnetospheric control of ionospheric TEC perturbations via whistler-mode and ULF waves," Sep. 08, 2024, *arXiv*: arXiv:2409.05168. doi: 10.48550/arXiv.2409.05168.
[27] Y. Ito *et al.*, "On the Factors Controlling the Relationship Between Type of Pulsating Aurora and Energy of Pulsating Auroral Electrons: Simultaneous Observations by Arase Satellite, Ground-Based All-Sky Imagers and EISCAT Radar," *J. Geophys. Res. Space Phys.*, vol. 129, no. 7, p. e2024JA032617, 2024, doi: 10.1029/2024JA032617.